ELSEVIER

Journal of Photochemistry and Photobiology A: Chemistry 127 (1999) 57–65

Journal of Photochemistry and Photobiology A:Chemistry

www.elsevier.nl/locate/jphotochem

Photochemistry of water-soluble quinones. Production of the hydroxyl radical, singlet oxygen and the superoxide ion

Antonio E. Alegría *, Amaris Ferrer, Glysette Santiago, Elsa Sepúlveda, Wilmarie Flores

Department of Chemistry, University of Puerto Rico at Humacao, Humacao, Puerto Rico 00791

Received 9 March 1999; accepted 15 June 1999

Abstract

Quantum yields for the photosensitized production of singlet oxygen and superoxide ion by the several quinones 1,4-benzoquinone, BQ, 2-methyl-1,4-benzoquinone, MBQ, sodium 1,4-naphthoquinone-2-sulfonate, NQ2S, sodium 9,10-anthraquinone-2-sulfonate, AQ2S, 1, 4-naphthoquinone, NQ, 2-hydroxy-1,4-naphthoquinone, LWQ, 5,8-dihydroxy-1,4-naphthoquinone, NZQ, 5-hydroxy-1,4-naphthoquinone, JQ, and disodium 9,10-anthraquinone-1,5-disulfonate, AQDS in aqueous buffer (pH 7), at wavelengths above 310 nm, have been determined. Quantum yields for the production of singlet oxygen were found to be smaller than that for the production of superoxide. The quantum yield for the production of the hydroxyl adduct of 5,5-dimethyl pyrroline-1-oxide, DMPO-OH, by NQ was also determined and was found to be oxygen-concentration-dependent while the photoproduction of this adduct by hydroxynaphthoquinones was not observed. Evidence was obtained which suggests that the observed DMPO-OH adduct is produced by the free hydroxyl radical, at least at low NQ concentration.

Keywords: Quinone photochemistry; Quantum yield; DMPO; Hydroxyl radical; Superoxide; Singlet oxygen

1. Introduction

Quinones play important roles in electron transfer in bacteria [1], photosystems of green plants [2] and mitochondria [3]. Although natural hydrophobic quinones such as ubiquinone and plastoquinone are found in organelles in which electron transport occurs, models have been created with these and other quinones to mimic photosynthesis [4,5] and cellular respiration [6].

Quinones and their reduced derivatives, the hydroquinones, have been used as electron acceptors and donors in photosynthetic models aimed at the conversion and storage of solar energy [4,5]. Since both naturally-occurring and artificial light conversion and storage, as well as redox, systems may be (or are) exposed to sunlight, understanding the photochemistry of quinones in these systems should be useful.

Some quinones are postulated as water-photooxidizing agents when irradiated in the visible or UV light ranges. The corresponding hydroquinones and monohydroxylated products are reported as the major photoproducts under anaerobic conditions [7–10]. Hydrogen peroxide is another major photoproduct in aerobic solutions. In general, the mechanism is postulated to involve the reaction of the quinone triplet state, or cation radical with water to produce the hydroxylating intermediate [7,11–17]. While unambiguous evidence was obtained by Bolton and coworkers in identifying the hydroxyl radical as the hydroxylating agent during the anaerobic photolysis of *p*-benzoquinone, BQ, [12] the identity of this intermediate is a matter of debate for other quinones such as anthraquinone sulfonates. Evidence has also been obtained in our laboratory which suggests that BQ and 2-methyl-1,4-benzoquinone, MBQ, but not 9,10-anthraquinone-1,5-disulfonate, AQDS, are able of photooxidizing water with the consequent production of the free OH radical [17].

In a previous work we reported the formation of a water-derived OH adduct of the spin trap, 5,5-dimethyl pyrroline-1-oxide (DMPO) obtained during the photolyses of water-soluble quinones [17]. Electron paramagnetic resonance (EPR) spectroscopic techniques are used in the present work to obtain information on the relative efficiency of production of this water-derived OH adduct for 1,4-naphthoquinone. The efficiencies of production of other reactive intermediates such as superoxide ion and singlet

* Corresponding author. Tel.: +787-852-3222; fax: +787-852-3222
E-mail address: a_alegria@cuhac.upr.clu.edu (A.E. Alegría)

1010-6030/99/$ – see front matter
PII: S1010-6030(99)00138-0

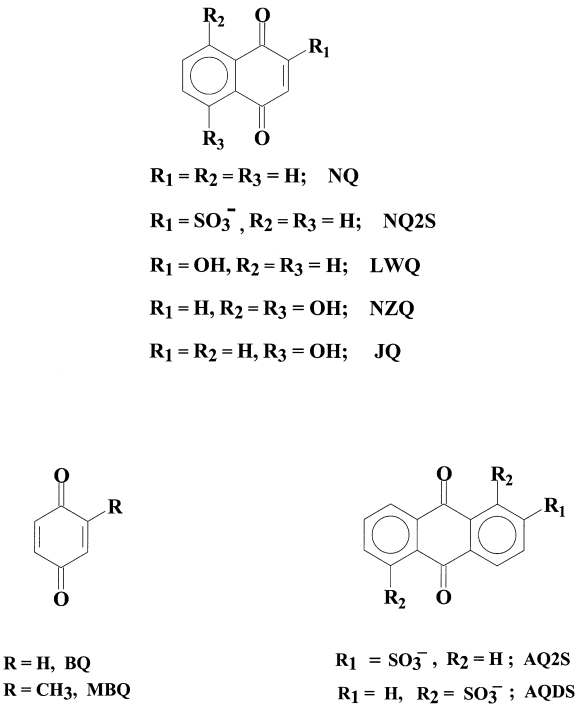

Fig. 1. Quinones under study in this work.

oxygen have been determined as well. Knowledge of the relative abilities of quinones for photo-producing reactive intermediates is needed in order to predict the importance of degrading reactions in energy-storing photosystems. We have limited these studies to irradiation wavelengths within the solar radiation range (>310 nm), due to the relevance of this region to solar energy harnessing models.

2. Experimental details

2.1. Chemicals

The quinones 1,4-benzoquinone, BQ (Pfaltz and Bauer), 2-methyl-1,4-benzoquinone, MBQ (Aldrich), sodium 1,4-naphthoquinone-2-sulfonate, NQ2S (Kodak), sodium 9,10-anthraquinone-2-sulfonate, AQ2S (Aldrich), 1,4-naphthoquinone, NQ (Baker), 2-hydroxy-1,4-naphthoquinone, LWQ (Sigma), 5,8-dihydroxy-1,4-naphthoquinone , NZQ (Sigma), 5-hydroxy-1,4-naphthoquinone, JQ (Sigma), and disodium 9,10-anthraquinone-1,5-disulfonate, AQDS (Aldrich) were obtained from several sources (Fig. 1). The quinones BQ, MBQ, NZQ, LWQ, JQ and NQ were purified by sublimation. The sulfonated quinones were purified by recrystallization from water/methanol mixtures. The spin trap, DMPO, was purchased from Sigma and distilled at low pressure prior to use (75°C at 0.5 Torr). All purified quinones were stored at 5°C protected from light. The hydroxylamine of 4-hydroxy-2,2,6,6-tetramethylpiperidine-1-oxyl, TEMPOL-H, was synthesized as described elsewhere by reduction of the corresponding nitroxyl radical precursor, TEMPOL, with hydrogen in the presence of platinum catalyst until less than 0.5% TEMPOL was detected as impurity utilizing EPR spectroscopy [18]. The compounds imidazole, 2,5-dimethylfuran (DMF) and *p*-nitrosodimethylaniline (RNO) were purchased from Sigma. Quinone stock solutions were prepared in distilled deionized water and used the same day. Quinones with low water solubility, i.e. NQ, NZQ and JQ were vortex-stirred in water, followed by centrifugation and the supernatant used as stock solution.

DMPO stock solutions were prepared in distilled deionized water and stored at −20°C protected from light. All manipulations were performed under minimized room light exposure. Samples were irradiated in 50 mM phosphate buffer solutions at pH 7.0.

^{17}O-enriched water (35 mol% ^{17}O) was purchased from ICON Services and stored in a sealed bottle inside a desiccator after used.

2.2. EPR measurements

Photolyses were performed either in situ, or outside the EPR instrument cavity at room temperature and at the corresponding wavelength maximum of each quinone ($\lambda > 310$ nm). For photolyses occurring inside the EPR cavity a quartz sample cell ($60 \times 10 \times 0.25$ mm) was used. A suprasil quartz cell with a 1.00 cm light path was used for photolyses occurring outside the EPR cavity followed by EPR analysis of the photolyte. A double resonator was used in the EPR instrument. A capillary tube containing an aqueous sample of $CuSO_4$ was left in the same position in one of the EPR instrument cavities and used to correct for cavity tuning irreproducibility [19]. A 1000 W xenon arc lamp coupled to a Schoeffel grating monochromator with a bandwidth of ±20 nm was used as the irradiation source.

EPR spectra were recorded on a Bruker ER-200D spectrometer at 100 kHz magnetic field modulation. Computer simulations of EPR spectra were made to match the observed one using WINSIM [20].

Anaerobic and oxygen-saturated experiments were carried out by saturating the quinone solutions with nitrogen or oxygen, respectively, in septum-stoppered test tubes and transferred to the EPR quartz cell with air-tight syringes. Air-saturated experiments were performed with the quartz cell opened to air at the top.

Radical concentrations were determined by comparison of their double integrated first derivative EPR signals with that of a 3-carbamoyl-2,2,5,5-tetramethyl-1-pyrrolidine-yloxy (CTPO) free radical standard. EPR line intensities were determined from the peak-to-peak derivative amplitudes times the square of the peak-to-peak widths of the mentioned EPR line and converted to concentration units using the double integrated total area of the spin adduct and that of CTPO. EPR line intensities determined in this manner were found to be directly proportional to the spin adduct double integrated total spectral area within ±4%.

Since the nitroxide concentration at the irradiation area in the EPR quartz cell is supposed to be higher immediately after photolysis, while the ferric oxalate actinometry, used to measure the rate of incident photons [21] is made of all the solution contained in the EPR quartz cell, nitroxide concentrations were corrected to obtain their concentrations after diffusing through the total volume of the EPR sample cell by photolyzing a dimethylsulfoxide sample containing 1% H_2O_2 and 3,5-dibromo-4-nitrosobenzene sulfonic acid (DBNBS) for 5 s, as described previously [17,22]. The double integrated areas of the corresponding stable DBNBS-CH_3 adduct EPR spectrum were measured immediately after homogenizing the nitroxide concentration throughout the flat cell solution. Thus, rates of nitroxide production were corrected by multiplying by the ratio of the DBNBS-CH_3 areas corresponding to after and before homogenizing the methyl adduct concentration.

2.3. Absorption spectra

These were measured using a Beckman DU 7400, diode array UV-Vis spectrophotometer.

2.4. Determination of the fraction of DMPO-OH which is derived from air

Air saturated aqueous solutions were prepared containing tenths of a milligram (weighed in a Cahn microbalance) of NQ, 10 μl of ^{17}O-enriched water (35% by O mol) and 0.2 μl of neat DMPO. This solution was transferred into a Pyrex capillary tube sealed at one extreme. The sample was then placed in the EPR instrument cavity and irradiated at the quinone maximum absorption wavelength until a good signal-to-noise ratio was achieved in the DMPO-OH EPR spectrum. The fraction of DMPO-OH which is derived from air was obtained using Eq. (1) [14,23],

$$\frac{[\text{DMPO-OH}]_{\text{air}}}{[\text{DMPO-OH}]_{\text{water}}} = f(x+1) - 1 \quad (1)$$

where x is the [DMPO-^{16}OH]/[DMPO-^{17}OH] ratio and f is the enrichment fraction of the ^{17}O-enriched water, i.e. 0.35 in this case. These 'x' values were estimated by varying the assumed spectral EPR parameters, using WINSIM, in order to optimize the match between calculated and experimental spectra. Experimental spectra were acquired using the acquisition software developed by Morse [24].The acquired data was imported into WINSIM for simulated spectra optimization.

2.5. Quantum yields for the production of DMPO-OH

These were determined as described previously [17], where the initial rates of increase in the line intensity of the first derivative $M_I = 1/2$ DMPO-OH EPR peak ($R_{DMPO\text{-}OH}$) is measured during the photolyses of solutions containing 100 mM DMPO and the corresponding quinone (Q). Quantum yields for the production of DMPO-OH ($\Phi_{DMPO\text{-}OH}$) were obtained by comparing the measured $R_{DMPO\text{-}OH}$ values with that corresponding to an air-saturated solution containing anthraquinone-2-sulphonate (AQ2S) and using the reported value of $\Phi_{DMPO\text{-}OH}$ for AQ2S (0.18, [17]) and the corresponding number of absorbed photons.

The rate of incident photons was calculated from the relative light energy flux, determined using an International Light radiometer model IL-1700 with an SED-033 probe coupled to ferric oxalate actinometry at 405 nm [21].

2.6. Quantum yields of superoxide formation, $\Phi(O_2^{\bullet-})$

It has been demonstrated that TEMPOL is produced from its hydroxylamine, TEMPOL-H, via oxidation by $O_2^{\bullet-}$ [25]. Thus we determined $\Phi(O_2^{\bullet-})$ values from the SOD-inhibitable rates of production of the one-electron oxidation product of TEMPOL-H instead of using the most used test for superoxide ion, i.e. the SOD-inhibitable ferricytochrome c reduction [26], since overlap exists between the soret band of this molecule and the absorbance maxima of some of the quinones under study here. Rates of TEMPOL formation were measured from the initial rates of increase in the line intensity of the lower field first derivative TEMPOL EPR peak in O_2-saturated solutions containing quinone and 20 mM TEMPOL-H. The reagents DTPA (100 μM) and $NaHCO_2$ (600 mM) were also added to avoid Fenton-type production of hydroxyl radicals and the subsequent degradation of TEMPOL-H. SOD-inhibitable rates of TEMPOL (R_{TEMPOL}) were obtained by subtracting initial average rates of line intensity increase in the presence of 200 units SOD/ml and 500 units catalase/ml to those obtained in the absence of these enzymes. Quantum yields for the production of superoxide, $\Phi(O_2^{\bullet-})$, were determined using Eq. (2), where R_{TEMPOL} is the SOD-inhibitable rate of TEMPOL formation by a given quinone, Q,

$$(\Phi)O_2^{\bullet-} = \frac{R_{\text{TEMPOL}}}{(1 - 10^{-A_Q})R_{\text{photon}}} \quad (2)$$

A_Q is the corresponding solution absorbance and R_{photon} is the rate of incident photons.

2.7. Quantum yields of $^1O_2$ formation, $\Phi(^1O_2)$

These were determined by the reaction of singlet oxygen with imidazole followed by the reaction of the transannular peroxide with RNO [27] only for quinones where no overlap occurs between quinone irradiation wavelengths and that of RNO (440 nm), i.e. AQ2S, AQDS, NQ and NQ2S. Consumption of RNO was measured at 440 nm after 5 min of irradiation of air-saturated quinone-containing samples at the quinone maximum absorption wavelengths and compared to that obtained during the irradiation of a RB solution. Quantum yields for the production of $^1O_2$ are obtained

using Eq. (3), where ΔA_Q (RNO) and ΔA_{RB} (RNO) are the absorbance decrease at 440 nm in 5 min corresponding to

$$\Phi_Q(^1O_2) = \frac{[\Delta A_Q(\text{RNO})][R_{\text{photon}}(\text{RB})][1-10^{-A(\text{RB})}]\Phi_{RB}(^1O_2)}{[\Delta A_{RB}(\text{RNO})][R_{\text{photon}}(\text{Q})][1-10^{-A(\text{Q})}]} \quad (3)$$

Q and RB, R_{photon} (Q)/R_{photon} (RB) is the ratio of the number of incident photons at the corresponding irradiation wavelengths of Q and RB and A_Q and A_{RB} are the corresponding absorbances. For quinones with irradiation wavelengths overlapping with 440 nm, i.e. BQ, LWQ, NZQ and JQ, singlet oxygen quantum yields were determined by reaction of the photoproduced singlet oxygen with 2,5-dimethylfuran, DMF [28] since DMF absorbance region (λ_{max} = 215 nm) does not interfere with quinones irradiation wavelengths. DMF consumption was followed by HPLC analysis. Quantum yields for the production of $^1O_2$ were obtained using Eq. (3), where ΔA (RNO) corresponding to quinone or RB is substituted by ΔA (DMF) which is the corresponding DMF chromatographic peak area decrease per minute of irradiation. In order to suppress quinone and DMF degradation by hydroxyl radicals 50 μM DTPA, 10 mM mannitol, 250 units of catalase/ml were added to samples used in singlet oxygen production determinations [29]. The reported literature value of Φ_{RB} ($^1O_2$) = 0.76 is used [30]. Photolyses were also carried out in the presence of D_2O and of 30 mM NaN_3 to test for the presence of $^1O_2$, since the former enhances $^1O_2$ lifetime [31], and thus Φ ($^1O_2$) values are expected to increase, and the latter quenches $^1O_2$ by collisional deactivation [32], thus decreasing singlet oxygen yields.

2.8. HPLC analyses

A Waters analytical HPLC system equipped with a 600 solvent delivery pump, UV–Vis tunable detector and a μBondapack C_{18}(3.9 × 300 mm) column was used. A mobile phase of MeOH/H_2O at a convenient volume ratio (depending on the sample mixture) was used at a flow rate of 1 ml/min. Detection of DMF was made at 230 nm.

3. Results and discussion

3.1. Fraction of DMPO-OH derived from air

Upon irradiating solutions containing DMPO and NQ in air-saturated ^{17}O-enriched water, an EPR spectrum is obtained where both [DMPO-^{16}OH] and [DMPO-^{17}OH] species are observed (Fig. 2). It can be easily deduced from a fast inspection of this spectrum that most of the DMPO-OH detected is derived from water. The same observation is made in the absence of air although a smaller yield of total DMPO-OH adducts is obtained (see below). An analogous observation has been detected previously for other quinones thus suggesting that this behavior is common to all types of water-soluble quinones [17]. From the simulated simultaneous EPR spectra, the corresponding [DMPO-^{16}OH]/[DMPO-^{17}OH] and $[\text{DMPO-OH}]_{air}/[\text{DMPO-OH}]_{water}$ ratios were found to be 1.3 ± 0.2 and -0.2 ± 0.3, respectively, indicating that all of the DMPO-OH adduct is derived from water.

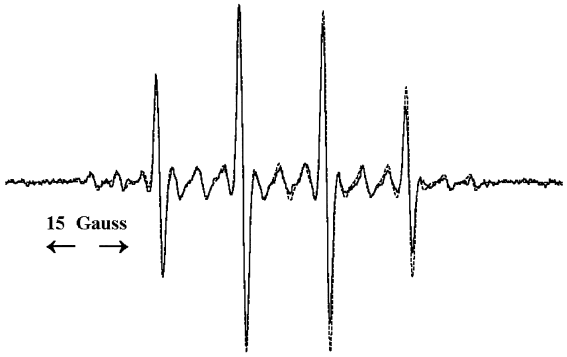

Fig. 2. First derivative EPR spectra observed during irradiation at 346 nm of an aqueous solution containing 10 μl of $H_2{}^{17}O$-enriched (35 % by O mol), NQ and 0.2 μl of neat DMPO. Both the experimental (——) and the calculated spectra (· · ·) are shown. Optimization of the calculated spectrum using WINSIM produced for DMPO-^{16}OH: relative abundance 56 %, a_N (1N) = 15.06 G, a_H (1H) = 14.79 G, linewidth = 0.57 G and for DMPO-^{17}O: relative abundance 44 %, a_N (1N) = 14.99 G, a_H(1H) = 14.60 G, $a_{^{17}O}$ = 4.66 G and linewidth 0.68 G. Relative abundance of each species are stated in the text. These coupling constants are similar to those assigned previously [14,45].

No DMPO-OH signal was detected during the irradiation of hydroxy-substituted quinones, not even if irradiated in a 1 cm suprasil cell outside the EPR instrument cavity followed by EPR analysis, although the absorbances of these quinone solutions were as large or higher than that of NQ. *Peri*-interactions in JQ and NZQ cause a red shift of the benzenoid absorption by virtue of strong intramolecular hydrogen bonding preventing photoreduction of quinones by hydrogen donors and, most probably, possible electron donors in our case such as DMPO, other quinone molecules or even water [33–35]. A high yield of S_1 to S_0 internal conversion has also been postulated to occur during the photolyses of the hydroxynaphthoquinones NZQ and JQ to explain the remarkable low yields of fluorescence and phosphorescence of these quinones, most probably caused by internal hydrogen bonding [36]. These two effects could also account for the undetectability of DMPO-OH during the photolyses of JQ and NZQ.

As indicated above, most of the observed DMPO-OH derives from water during the photolyses of NQ, AQ2S, naphthoquinone-2-sulphonate, NQ2S, 1,4-benzoquinone, BQ, methylbenzoquinone, MBQ and 2,6-anthraquinone-disulfonate, AQDS [17]. This was not necessarily expected since the quinone excited state could reduce oxygen to form the superoxide ion. The latter could either add to DMPO, governed by a rather small rate constant (17.9 M^{-1} s^{-1}), followed by decomposition to DMPO-OH [37] or dispro-

$$Q \xrightarrow{h\nu} Q^{*}$$
$$Q^{*} + O_2 \rightarrow Q^{+\bullet} + O_2^{\bullet-}$$
$$O_2^{\bullet-} + DMPO \rightarrow DMPO - O_2^{\bullet-}$$
$$DMPO - O_2^{\bullet-} \rightarrow\rightarrow DMPO - OH$$
$$2O_2^{\bullet-} + 2H^{+} \rightarrow H_2O_2 + O_2$$
$$Fe^{+3} + O_2^{\bullet-} \rightarrow Fe^{+2} + O_2$$
$$Fe^{+2} + H_2O_2 \rightarrow \bullet OH + OH^{-} + Fe^{+3}$$
$$Q^{*} + H_2O_2 \rightarrow Q^{+\bullet} + \bullet OH + OH^{-}$$
$$\bullet OH + DMPO \rightarrow DMPO - OH$$

Scheme 1.

portionate to hydrogen peroxide and oxygen. Hydrogen peroxide could generate OH radicals through reductive scission of its bond by a Fenton-type reaction [38] or through a photosensitized reduction by the quinone excited state. The generated OH radicals will add to DMPO governed by a high rate constant in the order of $10^9\,M^{-1}\,s^{-1}$[37]. The above-mentioned reactions are shown in Scheme 1. If superoxide ions are produced during the photolyses of these quinones, addition of either $O_2^{\bullet-}$ or OH (derived from H_2O_2) to DMPO are, evidently, not important pathways in the quinone-photosensitized production of DMPO-OH. A water-derived DMPO-OH adduct was also found to be produced almost exclusively during the photolyses of anthracycline quinones [14] and menadione [39] in air-saturated water.

Singlet oxygen could also induce the formation of DMPO-OH [40]. An exclusively air-derived DMPO-OH adduct was detected in that work. Although NQ could also photogenerate singlet oxygen, again, the contribution of singlet oxygen to DMPO-OH formation will also be very minor, if occurring at all, since DMPO-OH derives from water almost exclusively. However, this does not preclude the possibility of $^1O_2$ formation. In spite of their weak roles in the quinone-photosensitized production of DMPO-OH, both $O_2^{\bullet-}$ and $^1O_2$ production could still play important roles in the aqueous photochemistry of quinones.

3.2. Quantum yields for the formation of DMPO-OH

Three possibilities have been invoked regarding the activated species producing the hydroxylated quinone products. These are the hydroxylated quinone radical [7,15,16], excited quinone photosolvate [9] and the free hydroxyl radical [12,17]. The intermediacy of the adriamycin cation radical was postulated to explain the higher yields of DMPO-OH obtained in air as compared to nitrogen-saturated solutions [14]. Quantum yields for the production of DMPO-OH were also found to be larger in air than in N_2-saturated solutions of MBQ, AQ2S, NQ2S and AQDS [17]. A higher photoproduction of DMPO-OH was also observed during the photolysis of air-saturated solutions of menadione in the presence of DMPO as compared to in the absence of air [39].

In order to check if that behavior is extended to other water-soluble quinones, we measured the quantum yields for the production of DMPO-OH in the presence and absence of air. As mentioned earlier, no DMPO-OH signal could be detected for hydroxynaphthoquinones in the presence or absence of air and in the presence of 100 mM DMPO. In a previous work we have found that at this DMPO concentration a maximum amount of DMPO-OH adducts is produced, within experimental error, during the photolysis of AQ2S, a strong DMPO-OH generator, in air-saturated solution [17]. However, the values obtained of $R_{DMPO\text{-}OH}$ during the photolyses of N_2- and air-saturated solutions of NQ were $(1.9 \pm 0.4) \times 10^{-7}$ and $(3.1 \pm 0.5) \times 10^{-7}\,M\,s^{-1}$, respectively. Using these values, that corresponding to the photolysis of AQ2S in air-saturated water and the reported $\Phi_{DMPO\text{-}OH}$ value for AQ2S (0.18 ± 0.03) [17], the quantum yields for the production of DMPO-OH by NQ in air- and N_2-saturated aqueous solution is obtained, Table 1. Again, a smaller quantum yield for the production of DMPO-OH is detected during the photolysis of N_2-saturated as compared to air-saturated solutions of NQ. Two explanations have been proposed for this observation. In one of them, oxygen is enhancing the rate of formation of DMPO-OH by, presumably, oxidation of the quinone triplet or other quinone-derived transient intermediate (S) which acts as a more efficient DMPO hydroxylator or produce a DMPO hydroxylator at a higher rate [17], Eqs. (4) and (5). Another explanation proposes the

$$Q^{*} + O_2 \rightarrow S \quad (4)$$

$$S + H_2O + DMPO \rightarrow DMPO\text{-}OH \quad (5)$$

quinone-photosensitized oxidation of DMPO to produce the DMPO cation radical followed by reaction of the latter with water to produce DMPO-OH, Eqs. (6) and (7) [39,41]. In the latter

$$Q^{*} + DMPO \rightarrow DMPO^{\bullet+} + Q^{\bullet-} \quad (6)$$

$$DMPO^{\bullet+} + H_2O \rightarrow DMPO\text{-}OH \quad (7)$$

proposal, oxygen is oxidizing the semiquinone back to the quinone, thus, maintaining a higher quinone concentration as compared to the anaerobic photolysis with the consequent larger yields of DMPO-OH adduct. However, at present, the identities of these oxidized intermediates which promote an enhanced rate of DMPO hydroxylation, in the presence of air, during the photolyses of aqueous solutions of NQ and other water-soluble quinones have not been identified unambiguosly.

3.3. Is the free hydroxyl radical an intermediate in the DMPO-OH formation?

The kinetic competition between DMPO and other OH radical scavengers, such as ethanol or formate, has been previously used to establish or rule out the possibility of free

Table 1
Quantum yields for the production of DMPO-OH, $O_2^{\bullet -}$, and $^1O_2$ by the quinones under study in this work in aqueous buffer, pH 7

Quinone	λ/nm[f]	$\Phi_{DMPO\text{-}OH}$		$R(_{TEMPOL,Q}/10^{-8}\,M\,s^{-1})$[c]	$\Phi(O_2^{\bullet -})$[c]$/10^{-2}$	$\Phi(^1O_2)$
		N_2	Air			
BQ	424	0.13 ± 0.01[a]	0.13 ± 0.02[a]	1.5 ± 0.2	29 ± 4	0.14 ± 0.03[e]
MBQ	326	0.05 ± 0.03[a]	0.16 ± 0.03[a]	4.6 ± 3	6.2 ± 0.5	0.11 ± 0.06[d]
NQ	346	0.033 ± 0.006	0.054 ± 0.003	28 ± 2	5.9 ± 0.6	0.27 ± 0.07[d]
NZQ	486	[b]	[b]	0.42 ± 0.06	0.22 ± 0.03	0.20 ± 0.04[e]
JQ	422	[b]	[b]	1.2 ± 0.3	0.48 ± 0.12	0.14 ± 0.04[e]
LWQ	455	[b]	[b]	0.05 ± 0.04	0.003 ± 0.002	[g]
NQ2S	346	0.009 ± 0.002[a]	0.059 ± 0.005[a]	1.3 ± 0.1	0.34 ± 0.04	0.38 ± 0.09[d]
AQ2S	330	0.024 ± 0.012[a]	0.18 ± 0.03[a]	33 ± 4	4.4 ± 0.4	0.41 ± 0.07[d]
AQDS	324	0.018 ± 0.009[a]	0.079 ± 0.008[a]	7.8 ± 0.9	2.5 ± 0.3	0.35 ± 0.08[d]

[a] From [17].
[b] No DMPO-OH signal detected.
[c] In oxygen-saturated solutions
[d] Determined by using the rate of RNO bleaching at 440 nm.
[e] Determined by using the rate of DMF bleaching.
[f] Irradiation wavelength.
[g] No DMF consumption was detected even after 25 min of irradiation.

OH radical as the hydroxylating intermediate [12,42,43]. In particular, Ononye et al. were the first research group to use this technique, where a competition between formate and DMPO for OH radicals proved the intermediacy of these during the photolysis of BQ in water [12]. The following reactions will occur in an aqueous sample containing quinone, formate and DMPO, where the free hydroxyl radical has been generated:

$$OH^{\bullet} + DMPO \xrightarrow{k_8} DMPO\text{-}OH \quad (8)$$

$$OH^{\bullet} + HCO_2^- \xrightarrow{k_9} CO_2^{-\bullet} + H_2O \quad (9)$$

$$CO_2^{-\bullet} + DMPO \xrightarrow{k_{10}} DMPO\text{-}CO_2 \quad (10)$$

Thus, Eq. (11) will then be obeyed, where $R_{DMPO\text{-}OH}$ and $R_{DMPO\text{-}CO_2}$ are the corresponding initial rates of adduct formation and [DMPO-OH] and [DMPO-CO_2] are the initial concentrations of

$$\frac{k_8}{k_9} = \frac{R_{DMPO\text{-}OH}}{R_{DMPO\text{-}CO_2}} \times \frac{[HCO_2^-]}{[DMPO]} \quad (11)$$

the respective adducts. Initial rates are used to avoid photoreactions of the quinone with the spin adducts. Since k_8 values are in the range $2.1\text{–}3.4 \times 10^9\,M^{-1}\,s^{-1}$ (36, 42) and $k_9 = 2.9 \times 10^9\,M^{-1}\,s^{-1}$ [44], then k_8/k_9 will be in the range 0.7 to 1.2. Thus, for solutions containing equal concentrations of DMPO and formate, the adduct formation rates ratio should also be within this range if free OH is the only hydroxylating agent.

Formation rates of DMPO-OH and DMPO-CO_2 in these samples were measured as described in Experimental details section. A plot of [DMPO-OH]/[DMPO-CO_2] versus $I_{DMPO\text{-}OH}/I_{DMPO\text{-}CO_2}$ was used to interpolate the corresponding concentration ratio for each $I_{DMPO\text{-}OH}/I_{DMPO\text{-}CO_2}$ ratio measured, as described previously [17], and from these data, the ratio of the initial rates of formation of the corresponding spin adducts, $R_{DMPO\text{-}OH}/R_{DMPO\text{-}CO_2}$, were obtained at different NQ concentrations (Fig. 3).

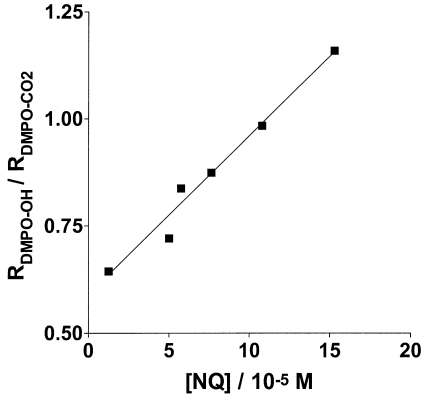

Fig. 3. Dependence of $R_{DMPO\text{-}OH}/R_{DMPO\text{-}CO_2}$ on quinone concentration during the photolyses of phosphate buffered (50 mM, pH 7) nitrogen-saturated solutions containing NQ, 100 mM DMPO and 100 mM sodium formate. The intercept is 0.6 ± 0.1.

This ratio decreases with a decrease in quinone concentration. A similar situation was observed previously for all the other quinones under study here with the exception of hydroxynaphthoquinones [17]. An analogous observation was also made by Ononye et al. during the photolyses of aqueous solutions of BQ in the presence of DMPO [12] and was explained by postulating a change in the DMPO-hydroxylating species as a function of quinone concentration. A hydroxyl exchange reaction between the monohydroxylated benzoquinone radical (produced by OH addition to the quinone) and DMPO has been proposed by Ononye et al. to occur preferentially at larger concentrations of quinone, while at infinite low quinone concentrations the free hydroxyl radical reaction with DMPO is preferred [12]. A hydroxylating agent, presumably Q-OH^- or Q-$OH^{\bullet}$, designated as intermediate 'C', is postulated as the quinone hydroxylator for AQ2S [15]. A water-quinone charge transfer complex

of anthraquinone-2,6-disulfonate, AQ26DS, at neutral pH is postulated as a precursor of the hydroxylated quinone radical intermediate in the photolysis of this quinone [16]. However, another species designated as 'B' is also postulated to form from the reaction of the triplet state of these sulfonated anthraquinones and water. A quinone photosolvate, AQ26DS... H_2O, has also been postulated as the precursor of the corresponding quinone hydroxylated radical, AQ26DS-$OH^{\bullet}$ [9]. Furthermore, as indicated above, hydrolysis of the DMPO cation radical to produce DMPO-OH has been proposed as the cause for this spin adduct in the presence of menadione or BQ [39]. Thus, either one or a combination of these possibilities, could also apply here as the cause for DMPO hydroxylation. The dependence of the adduct rates of formation ratios on NQ concentration, however, could imply that the DMPO-hydroxylator (or the DMPO-hydroxylating reaction) is changing of identity, including the free OH radical formation.

The intercept in Fig. 3, stated in the corresponding figure caption, is, within experimental error, within the 0.7 to 1.2 range indicated above, thus suggesting that NQ is producing the free OH radical in nitrogen-saturated aqueous buffer. In a previous work, the intercept (0.7 ± 0.2) as well as the points in a similar graph corresponding to the photolysis of H_2O_2, a typical free OH radical-producing system, were all within the free OH range as expected [17]. Using this competition technique, evidence was previously obtained suggesting that BQ and MBQ, but not AQDS, are able of photooxidizing water, with the consequent production of the free OH radical [12,17].

3.4. Quantum yields of superoxide formation

Photolysis of an oxygen-saturated solution of AQ2S in the presence of 20 mM TEMPOL-H produces an increase in TEMPOL concentration with time. A smaller rate of TEMPOL formation is detected in the presence of SOD (Fig. 4 (a)). The selected TEMPOL-H concentration is able to react with essentially all the superoxide ions generated by the quinone which produces the highest quantity of this species, i. e. 1 mM AQ2S, since no increase in the TEMPOL rate of production is detected above this TEMPOL-H concentration (Fig. 4 (b)). A similar behavior is observed for other quinones under study here. Values of SOD-inhibitable rates of TEMPOL formation and $\Phi(O_2^{\bullet -})$ are shown on Table 1. Again, small yields of superoxide are obtained from the irradiation of solutions containing hydroxynaphthoquinones as compared to those produced by other quinones. A salient feature of these data is the high $\Phi(O_2^{\bullet -})$ value observed for BQ as compared to other quinones in this work.

3.5. Quantum yields of $^1O_2$ formation

In the presence of D_2O or 30 mM NaN_3 an increase and a decrease is observed in the extents of DMF (or RNO) destruction, respectively, for almost all the quinones under study here, Table 2, thus indicating that the measured DMF (or RNO) consumption is due to the photosensitized production of $^1O_2$. Different enhancements of singlet oxygen production upon substitution of H_2O by D_2O were detected for the different quinones under study here. These differences should be caused by the different rates of singlet oxygen formation which depend basically on quinone concentrations, their absorption coefficients and singlet oxygen quantum yields. However, different concentrations of H_2O in these solutions, ranging from 1 to 5% by volume should affect the singlet oxygen lifetime, thus contributing also to the observed differences. In any case, the observed enhancements in substrate destruction rates strongly suggest singlet oxygen photoproduction.

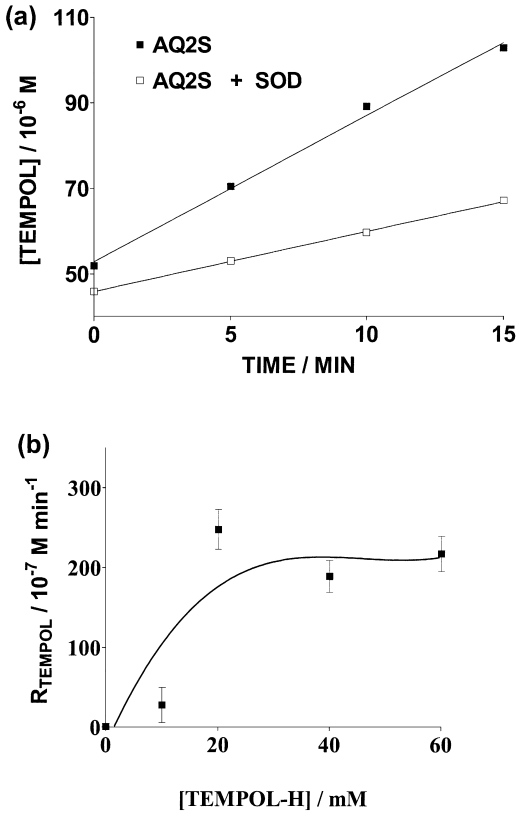

Fig. 4. (a) Effect of SOD addition on the rate of photooxidation of TEMPOL-H. The solution represented by empty squares contains AQ2S, 20 mM TEMPOL-H, 100 μM DTPA and 600 mM $NaHCO_2$ while that represented by full squares contains, in addition, 200 units SOD/ml and 500 units catalase/ml. (b) Dependence of the rate of TEMPOL-H oxidation on TEMPOL-H concentration upon irradiation of an oxygen-saturated solution containing AQ2S, 100 μM DTPA and 600 mM $NaHCO_2$and TEMPOL-H.

No solvent dependence in the rate of DMF consumption was detected during the irradiation of BQ in the presence of DMF. This is probably due to an enhanced destruction of this quinone by singlet oxygen in D_2O. However, a competition experiment was performed to obtain the rate constant for the quenching of $^1O_2$ by N_3^- as another evidence for the formation of $^1O_2$ by BQ. A plot of the inverse of the DMF

Table 2
Quinone photosensitized RNO or DMF consumption in the presence of either D_2O or NaN_3 in air-saturated 50 mM phosphate buffer at pH 7.0 relative to that observed in the absence of these reagents in water[a]

Quinone	MBQ[a]	NQ2S[a]	AQ2S[a]	AQDS[a]	NQ[a]	NZQ[c]	JQ[c]
$+D_2O$[b]	1.7	7.9	2.3	1.6	1.3	2.3	7.3
+30 mM NaN_3	0.31	0.22	0.78	0.20	0.59	0.25	0.54

[a] Values are the corresponding $\Delta A_Q(\mathrm{RNO})_{\mathrm{w\ D_2O\ (or\ w\ NaN_3)}} / \Delta A_{RB}(\mathrm{RNO})_{\mathrm{wo\ D_2O\ (or\ wo\ NaN_3)}}$ ratios at five minutes of irradiation time.
[b] Samples contained not less than 95 % (v/v) D_2O.
[c] Values are the corresponding $\Delta A_Q(\mathrm{DMF})_{\mathrm{w\ D_2O\ (or\ w\ NaN_3)}} / \Delta A_{RB}(\mathrm{DMF})_{\mathrm{wo\ D_2O\ (or\ wo\ NaN_3)}}$ ratios.

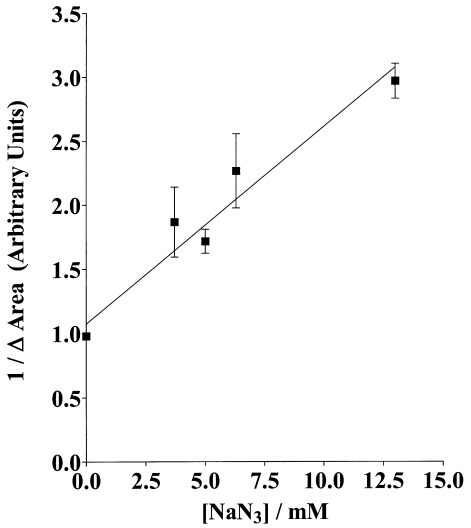

Fig. 5. Effect of NaN_3 addition on the chromatographic peak area of DMF (ΔArea) determined after five minutes of irradiation at 346 nm of an air-saturated sample containing 500 μM BQ and 1 mM DMF in 50 mM phosphate buffer (pH 7).

chromatographic peak area decrease per minute of irradiation (ΔA_{DMF}) vs. NaN_3 concentration produces a straight line from which the ratio of its slope to its intercept is equal to $k_{N_3^-}/(k_{DMF}\,[DMF])$ [46], where $k_{N_3^-}$ and k_{DMF} are the rate constants for the quenching of singlet oxygen by N_3^- and DMF, respectively (Fig. 5). A value of $1.5 \times 10^2\ M^{-1}$ was obtained for that ratio. Thus, using the reported value for k_{DMF} of $1.5 \times 10^9\ M^{-1}\ s^{-1}$ [47], $k_{N_3^-} = 2.3 \times 10^8\ M^{-1}\ s^{-1}$ is obtained which is close to that reported for aqueous solutions at neutral pH and ambient temperature ($4.5 \times 10^8\ M^{-1}\ s^{-1}$ [48]).

Quantum yields for the production of $^1O_2$ are shown on Table 1. Again, hydroxynaphthoquinones show the smallest quantum yields of singlet oxygen production. Larger Φ ($^1O_2$) values are also observed for sulfonated quinones than for the other types of quinones.

4. Conclusions

Quantum yields for the photosensitized production of singlet oxygen and superoxide ion by several quinones in aqueous buffer (pH 7), at wavelengths above 310 nm, have been determined. The quantum yield for the production of the DMPO-OH adduct by NQ was also determined and was found to be oxygen-concentration-dependent while the photoproduction of this adduct by hydroxynaphthoquinones was not observed. Evidence was obtained which suggests that the observed DMPO-OH adduct is produced by the free hydroxyl radical, at least at low NQ concentration. Smaller quantum yield values for the production of superoxide ions were also observed upon irradiation of hydroxynaphthoquinones as compared to those obtained for other types of quinones. Therefore, hydroxynaphthoquinones could be a convenient choice to be used in artificial solar energy storing devices in order to avoid undesirable system free radical degradation.

Acknowledgements

The authors are grateful to the National Science Foundation for supporting this work with grant No. CHE-9522623 and to NIH/NIGMS/MBRS and NSF/CIRE for partial support of this work with grants no. SO6-GM08216 and DMR-9872689, respectively. We are also grateful to Dr. Murali Krishna from NIH for helpful discussions.

References

[1] M.Y. Okamura, G. Feher, Adv. Photosynth. 2 (1995) 577.
[2] W. Maentele, in: M. Peirard (Ed), Nonlinear Excitations in Biomolecules, Springer, Berlin, 1995, pp. 295–316.
[3] H. Nohl, L. Gille, K. Staniek, Ann. N. Y. Acad. Sci. 854 (1998) 394.
[4] G. Tollin, in: H. Scheer (Ed), Chlorophylls, CRC Press, Boca Ratón, 1991, pp. 317–331.
[5] G. Steinberg-Yfrach, J.L. Rigaud, E.N. Durantini, A.L. Moore, D. Gust, T.A. Moore, Nature 392 (1998) 479.
[6] K. Krab, J. Bioenerg. Biomembr. 27 (1995) 387.
[7] P. Clark, H.I. Stonehill, J. Chem. Soc. Faraday Trans 1 68 (1972) 1676.
[8] S. Hashimoto, K. Kano, H. Okamoto, Bull. Chem. Soc. Japan 45 (1972) 966.
[9] H. Harriman, A. Mills, Photochem. Photobiol. 33 (1981) 619.
[10] K.C. Kurien, P.A. Robins, J. Chem. Soc. B. (1970) 855.
[11] M. Shirai, T. Awatsuji, M. Tanaka, Bull. Chem. Soc. Japan 48 (1975) 1329.
[12] A.I. Ononye, A.R. McIntosh, J.R. Bolton, J. Phys. Chem. 90 (1986) 6266.
[13] C.R. Burchill, D.M. Smith, J.L. Charlton, Can. J. Chem. 54 (1976) 505.
[14] A.E. Alegría, P. Riesz, Photochem. Photobiol. 48 (1988) 147.
[15] I. Loeff, A. Treinin, H. Linschitz, J. Phys. Chem. 87 (1983) 2536.

[16] D. Phillips, J.N. Moore, R.E. Hester, J. Chem. Soc. Faraday Trans. 2 82 (1986) 2093.
[17] A.E. Alegría, A. Ferrer, E. Sepúlveda, Photochem. Photobiol. 66 (1997) 436.
[18] J.B. Mitchell, A. Samuni, M.C. Krishna, W.G. DeGraff, M.S. Ahn, U. Samuni, A. Russo, Biochemistry 29 (1990) 2802.
[19] A. E Alegría, S. Rivera, M. Hernández, R. Ufret, M.. Morales, J. Chem. Soc. Faraday Trans. 89 (1993) 3773.
[20] D.R. Duling, J. Mag. Reson Ser. B 104 (1994) 105.
[21] J.G. Calvert, J.N. Pitts, Jr., Photochemistry, Wiley, New York, 1967.
[22] A.E. Alegria, C.M. Krishna, R.K. Elespuru, P. Riesz, Photochem. Photobiol. 49 (1989) 257.
[23] A.E. Alegria, O. Cox, J.A. Dumas, L.A. Rivera, P. Riesz, Biochim. Biophys. Acta 967 (1988) 1.
[24] P.D. Morse II, Meth. Enzymol. 127 (1986) 239.
[25] G.M. Rosen, E. Finkelstein, E.J. Rauckman, Arch. Biochem. Biophys. 215 (1982) 367.
[26] I. Fridovich, in: R.A. Greenwald (Ed.), Handbook of Methods for Oxygen Radical Research, CRC Press, Boca Raton, 1985, pp. 51–53.
[27] J.B. Verhalc, A. Gaudemer, I. Kraljić, Nouv. J. Chim. 8 (1984) 401.
[28] Y. Usui, K. Kamogawa, Photochem. Photobiol. 19 (1974) 245.
[29] M. Linetsky, B.J. Ortwerth, Photochem. Photobiol. 63 (1996) 649.
[30] P.C. Lee, M.A. Rodgers, Photochem. Photobiol. 45 (1987) 79.
[31] P. Bilski, B.M. Kukielczak, C.F. Chignell, Photochem. Photobiol 68 (1998) 675.
[32] K. Gollnick, D. Haish, G. Schade, J. Am. Chem. Soc. 94 (1972) 1742.
[33] J.M. Malcolm, in: S. Patai (Ed.), The Chemistry of Quinonoid Compounds, Wiley, London, 1974, Part 1, Chap. 9.
[34] I. Singh, R.T. Ogata, R.E. Moore, C.W. Chang, P. Scheuer, Tetrahedron 24 (1968) 6053.
[35] J.M. Bruce, K. Dawes, J. Chem. Soc. (C) (1970) 645.
[36] D.K. Palit, P. Haridas, T. Mukherjee, J.P. Mittal, J. Chem. Soc., Faraday Trans. 86 (1990) 3861.
[37] E. Finkelstein, G.M. Rosen, E.J. Rauckman, J. Am. Chem. Soc. 102 (1980) 4994.
[38] B.H.J. Bielski, Ann. Neurol. 32 (1992) 528.
[39] S. Monroe, S.S. Eaton, Arch. Biochem. Biophys. 329 (1996) 221.
[40] P. Bilski, K. Reszka, M. Bilska, C.F. Chignell, J. Am. Chem. Soc. 118 (1996) 1330.
[41] L. Eberson, J. Chem. Soc. Perkin Trans. 2 (1994) 171.
[42] K.M. Morehouse, R.P. Mason, J. Biol. Chem 263 (1988) 1204.
[43] P.R. Marriot, M.J. Perkins, D. Griller, Can. J. Chem. 58 (1980) 803.
[44] E. Farhataziz, A.B. Ross, Natl. Stand. Ref. Data Ser. 59 (1977).
[45] R.V. Lloyd, P.M. Hanna, R.P. Mason, Free. Radic. Biol. Med. 22 (1997) 885.
[46] Y. Lion, E. Gandin, A.V. Vorst, Photochem. Photobiol. 31 (1980) 305.
[47] Y. Usui, K. Kamogawa, Photochem. Photobiol. 19 (1974) 245.
[48] S. Miskoski, N.A. Garcia, Photochem. Photobiol. 57 (1993) 447.